Deadbeat Control with Parameter Identification under Single Phase-Shift Modulation for Dual Active Bridge Converters

Tan-Quoc Duong[1] and Sung-Jin Choi[2], *Member, IEEE*
[1,2]Department of Electrical, Electronic and Computer Engineering, University of Ulsan, Ulsan, South Korea
Email: [1]duongtanquoc@gmail.com, [2]sjchoi@ulsan.ac.kr

***Abstract*—This paper proposes a deadbeat control with parameter identification under single phase-shift modulation which aims to improve the output voltage regulation of dual active bridge converters. The least-squares analysis method is used to identify the actual values of parameters consisting of inductor and capacitor. In practice, the inductor and capacitor can vary due to tolerance and operation conditions, which cause regulation degradation. The proposed deadbeat parameter identification control is adopted to provide the predicted phase-shift angle accurately. When compared with the deadbeat control without parameter identification and conventional proportional-integral control under single phase-shift modulation, the steady-state performance and transient dynamic response of the output voltage of the proposed method are significantly improved. Simulation and experimental prototype setup are implemented to validate the advantages of the proposed method.**

Keywords—Deadbeat control, Dual active bridge, Single phase-shift, Parameter identification.

I. Introduction

Nowadays, more and more battery energy storage systems (BESS) are integrated into the dc microgrid, which presents a series of challenges for stable operation, safety, and the economics of the dc microgrid. One of the DC-DC converters that can capable charge and discharge the battery is the dual active bridge (DAB) converter because of its advantages such as simplicity, efficiency, and versatility of control [1], [2].

Some of the most important issues in a DC microgrid are stabilizing the output voltage, reducing the steady-state error, and achieving a rapid transient dynamic response under different operating modes. Many control methods have been introduced to control the output voltage, such as conventional proportional-integral (PI) control [3]–[5], model-based phase-shift control [6], feedforward control [7], model predictive control (MPC) [10]–[13], peak current control [12], and current stress optimization control [11], [13]–[19]. All of these methods stabilize and improve the performance of the output voltage using a simplified average model or an accurate model with fixed model parameters. However, they do not consider that the model parameters show tolerance to some extent and can even vary during operation. In practical experiments, the inductance and capacitance values can change concerned to manufacturing tolerance, temperature drift, aging, vibration, and stress. Thus, they can cause mismatches up to 20% when the actual values differ from the original values [20]–[23]. Consequently, the mismatches between model parameters and actual values of the inductance and output capacitance are inevitable in practice. Thus, reducing the sensitivity of parameter mismatch is considered to be an important issue [24], [25].

To address the parameter identification problem, the recursive least squares (RLS) method with model-based feedforward control can be used to enable online inductance identification [25]. However, it does not include the output capacitance, which also affects the performance of the output voltage. Furthermore, the RLS method is rather complicated as it contains many calculation steps and an additional PI control is used to directly control the phase-shift duty ratio, which can be subject to overcompensation under a large change in the feedforward signal, resulting in performance degradation. Another approach involves the adaptive online parameter identification algorithm defined in [26], which uses MPC and least-squares estimation to find the solution to the error function. However, in the paper, the least-squares solution was found by solving a 3–by–3 matrix, although there are only two variables that need to be found, so the calculation becomes too complex.

Besides, compared with other methods, deadbeat control is emerging as an effective way to control the output voltage of the DAB converters [27], [28]. However, these papers required midpoint current sampling, resulting in difficulty in real implementations. Moreover, in these papers, the changes in the value of the series inductor may cause performance degradation.

From the aforementioned analysis, this paper proposes a deadbeat control with parameter identification which aims to improve the output voltage regulation of the DAB converter. The least-squares analysis (LSA) is used to find the optimal solution of a set of linear equations to identify the actual values of the inductor and output capacitor. Besides, in order to control the output voltage of the DAB converter, single phase-shift (SPS) is one of the simplest modulations and is most widely adopted compared with the extended phase-shift (EPS), dual phase-shift (DPS), or triple phase-shift (TPS). Therefore, SPS modulation is used in this paper to demonstrate the effectiveness of the proposed idea.

This paper is divided into five sections. Deadbeat control under the SPS modulation scheme is briefly reviewed in Section II. In Section III, the proposed method is presented to identify parameters online including the inductor and output capacitor. Simulation and experimental comparison results are discussed in Section IV to illustrate the advantages of the proposed method in steady-state performance and transient

978-1-6654-0688-8/22/$31.00 ©2022 IEEE

dynamic response. Finally, Section V provides the conclusion.

II. Deadbeat Control under SPS Modulation

The DAB converter is shown in Fig. 1, which is composed of two active bridges interfaced through a high-frequency transformer (turn ratio n:1). The series inductance L_k consists of the transformer leakage inductance and extra inductance. Under SPS modulation, each bridge is regulated by a constant duty cycle of 50% to generate a high-frequency square-wave voltage between two active bridges.

The waveforms of the DAB converter under SPS modulation are shown in Fig. 2, including primary voltage v_p, secondary voltage v_s, inductor current i_L, phase-shift angle δ, and switching frequency f_s. For more simplified analysis, δ is chosen in the range of $[0 \sim \pi/2]$. Compared with other models such as the discrete-time model [29] or generalized average model [30], the reduced-order model [9], [12] has a good compromise in accuracy and complexity, thus, it is used in this paper. When the power flows from the input voltage side to the output voltage side, the secondary current is obtained as follows

$$i_s = \frac{n v_1 \delta \left(1 - \frac{\delta}{\pi}\right)}{2\pi f_s L_k}. \tag{1}$$

The dynamic equation of the output voltage is discretized according to the forward Euler approximation and derived as follows [8], [9]

$$v_2[k] = v_2[k-1] + \frac{i_s[k-1] - i_2[k-1]}{f_s C_2}, \tag{2}$$

where $v_2[k]$ and $v_2[k-1]$ are the output voltage at the k^{th} and $(k-1)^{th}$ sampling period, respectively; $i_s[k-1]$ and $i_2[k-1]$ are the secondary current and output current at the $(k-1)^{th}$ sampling period, respectively.

From (1) and (2), the output voltage is rewritten as follows

$$v_2[k] = \frac{n v_1[k-1]\delta[k-1]\left(1 - \frac{\delta[k-1]}{\pi}\right)}{2\pi f_s^2 L_k C_2} - \frac{i_2[k-1]}{f_s C_2} + v_2[k-1], \tag{3}$$

where $v_1[k-1]$ and $\delta[k-1]$ are the input voltage and phase-shift angle at the $(k-1)^{th}$ sampling period.

Aiming to control the output voltage equal to reference value $v_2 = v_{2ref}$, the predicted phase-shift angle at the k^{th} sampling period is derived as follows

$$\delta[k] = \pi\left(\frac{1}{2} - \left(\frac{1}{4} + 2n v_1[k] f_s^2 L_k \psi\right)^{1/2}\right), \tag{4}$$

where

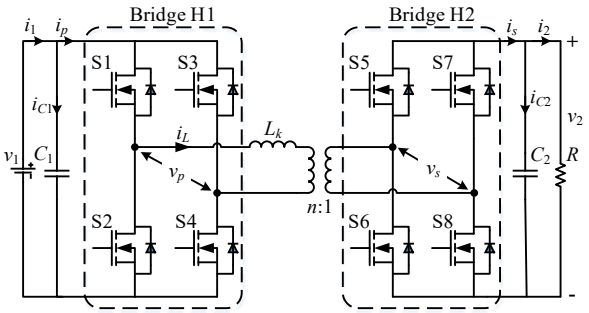

Fig. 1. Topology of the DAB Converter.

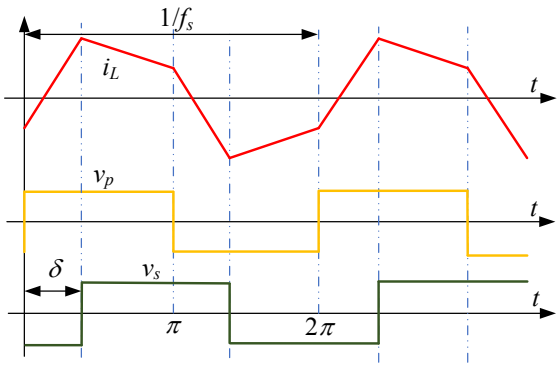

Fig. 2. Waveforms of the DAB converter under SPS modulation.

$$\psi = -\frac{i_2[k]}{f_s} - C_2 v_{2ref} + C_2 v_2[k]. \tag{5}$$

The equation (4) represents deadbeat control in which the optimal value of the phase-shift angle is directly derived from the values of system parameters (L_k and C_2) and measured values of voltage and current. That means the optimal value of the phase-shift angle strongly depends on system parameters.

The simulation results of the effects of parameter mismatches in deadbeat control without parameter identification are shown in Fig. 3 with simulation parameters are listed in Table I. it is easy to see that, when parameters vary in the range of 20% as mentioned in Section I, the output voltage has the steady-state error. In matched case (both L_k and C_2 have the values of 100% of their nominal values) from 0.03 (s) to 0.05 (s), steady-state error of the output voltage is immediately mitigated, and thus the output voltage v_2 completely coincides with the reference value v_{2ref}. From 0.05 (s) to 0.07 (s), the difference is about 0.4 V when both L_k and C_2 have values of 80% of their nominal values. When the value of L_k is greater than the nominal value, the output voltage v_2 is higher than the reference value v_{2ref}. Other mismatch cases also show the steady-state error of the output voltage.

From the aforementioned discussions, it can be seen that if the system parameters have mismatches, they cause the poor steady-state performance of the output voltage. Therefore, a simple method of parameter identification proposed in the next section will solve this problem.

III. Proposed Deadbeat Parameter Identification Control

To get the actual values of the parameter after every sampling period, (3) is rewritten as follows

$$v_2[k] = v_2[k-1] + \nu C[k-1] + \gamma D[k-1], \tag{6}$$

where

$$\begin{aligned} C[k-1] &= \frac{n v_1[k-1]\delta[k-1]\left(1-\frac{\delta[k-1]}{\pi}\right)}{2\pi f_s^2}, \\ D[k-1] &= -\frac{i_2[k-1]}{f_s}, \\ \nu &= \frac{1}{L_k C_2}, \\ \gamma &= \frac{1}{C_2}. \end{aligned} \tag{7}$$

Converting (6) to matrix form, it is obtained that

$$\boldsymbol{A}\boldsymbol{x} = \boldsymbol{B}, \tag{8}$$

where

$$\begin{aligned} \boldsymbol{A} &= \begin{bmatrix} C[k-1] & D[k-1] \\ C[k-2] & D[k-2] \\ \vdots & \vdots \\ C[1] & D[1] \end{bmatrix}_{(k-1)\times 2}, \\ \boldsymbol{x} &= \begin{bmatrix} \nu \\ \gamma \end{bmatrix}_{2\times 1}, \\ \boldsymbol{B} &= \begin{bmatrix} v_2[k]-v_2[k-1] \\ v_2[k-1]-v_2[k-2] \\ \vdots \\ v_2[2]-v_2[1] \end{bmatrix}_{(k-1)\times 1}. \end{aligned} \tag{9}$$

In order to find the optimal solution of (8), $\boldsymbol{x}$ is obtained by differentiating $\|\boldsymbol{A}\boldsymbol{x}-\boldsymbol{B}\|^2$ to zero as follows [31]

$$\begin{aligned} &\frac{\partial\left(\|\boldsymbol{A}\boldsymbol{x}-\boldsymbol{B}\|^2\right)}{\partial \boldsymbol{x}} = \boldsymbol{0} \\ &\Rightarrow \boldsymbol{x} = \left(\boldsymbol{A}^T\boldsymbol{A}\right)^{-1}\boldsymbol{A}^T\boldsymbol{B} = \left(\boldsymbol{N}\right)^{-1}\boldsymbol{M}, \end{aligned} \tag{10}$$

where

$$\begin{aligned} \boldsymbol{N} &= \begin{bmatrix} n_{11} & n_{12} \\ n_{21} & n_{22} \end{bmatrix} = \boldsymbol{A}^T\boldsymbol{A}, \\ \boldsymbol{M} &= \begin{bmatrix} m_1 \\ m_2 \end{bmatrix} = \boldsymbol{A}^T\boldsymbol{B}. \end{aligned} \tag{11}$$

Although matrix $\boldsymbol{A}$ and vector $\boldsymbol{B}$ have a large size, the sizes of matrix $\boldsymbol{N}$ and vector $\boldsymbol{M}$ are only 2–by–2 and 2–by–1, respectively. As a result, the calculated time is reduced by a simple 2–by–2 inverse matrix calculation. Fig. 4 shows the block diagram of the proposed method. Firstly, parameter identification is performed from (7)–(11). When the number of the sampling periods is increased, values of L_k and C_2 are

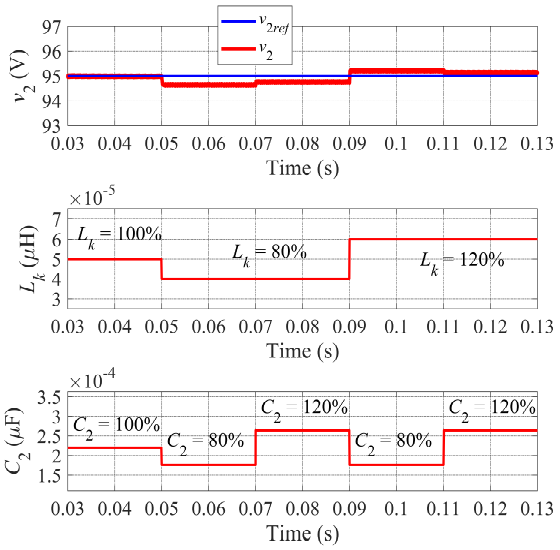

Fig. 3. Effects of parameter mismatches of deadbeat control without parameter identification.

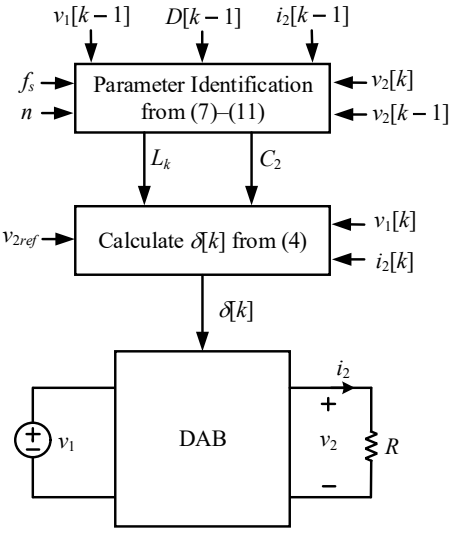

Fig. 4. Block diagram of the proposed method.

TABLE I
Parameters

Parameters	Symbol	Values
Input voltage	v_1	100 V
Reference value of the output voltage	v_{2ref}	95 V
Switching frequency	f_s	10 kHz
Transformer turn ratio	n	1
Series inductor	L_k	51 μH
Output capacitor	C_2	219 μF
Resistor load	R	20 Ω

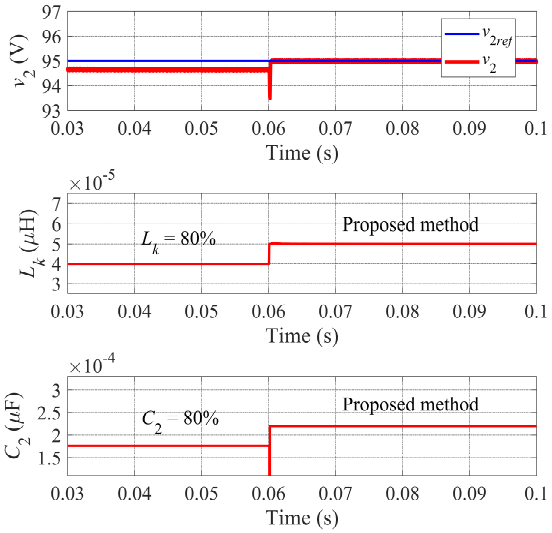

Fig. 5. Simulation results when the proposed method is applied at 0.06 (s).

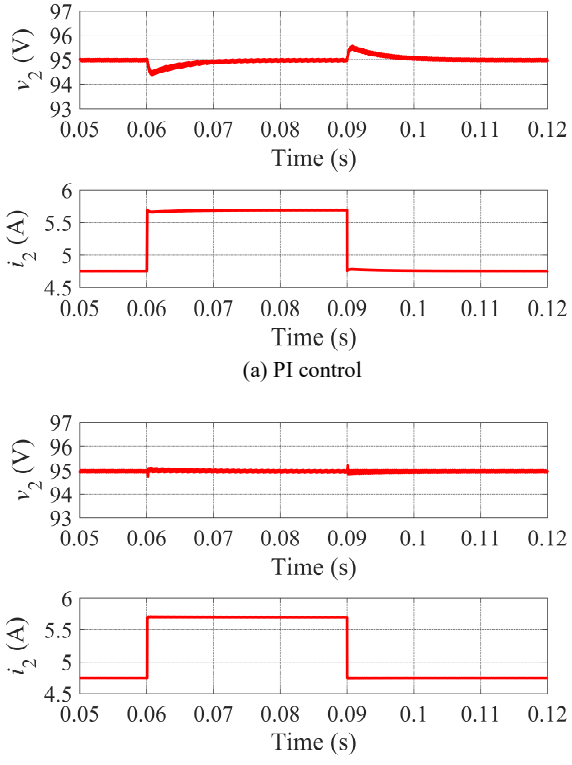

(a) PI control

(b) Proposed method

Fig. 6. Simulation results when the output current i_2 changes from 4.75 A to 5.7 A.

easily derived. Then, the predicted phase-shift angle δ is derived with deadbeat control as shown in (4). Since parameters are identified accurately, the output voltage v_2 also traces v_{2ref} accurately.

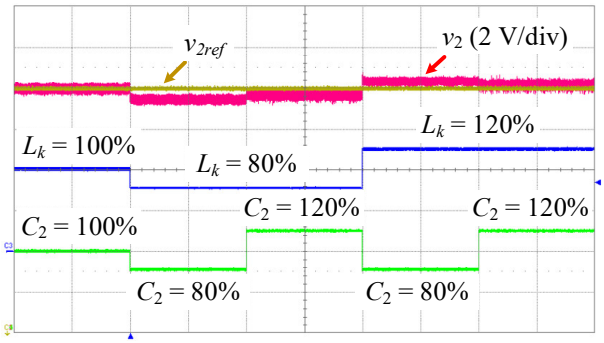

(a) Effects of parameter mismatches of deadbeat control without parameter identification

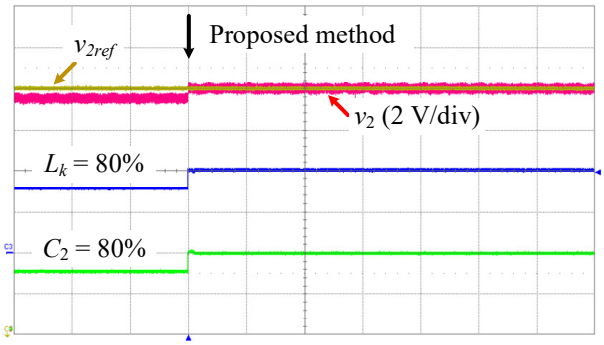

(b) Proposed method

Fig. 7. Experimental results (50 ms/div).

IV. Simulation and Experimental Results

The simulation results of the proposed deadbeat parameter identification control (proposed method) are shown in Fig. 5. Firstly, deadbeat control without parameter identification is implemented with L_k and C_2 underestimated by 80% of their nominal values, the same issue has occurred as shown in Fig. 3. At 0.06 (s), when the proposed method is applied, the parameters L_k and C_2 are converged quickly to actual values after a few sampling periods, and the output voltage traces reference value accurately.

In this paper, the proposed method is compared with the conventional PI method under SPS modulation to show its advantages. The PI controller is designed with a phase margin of 90 degrees and a target gain cross-over frequency f_c = 2000 Hz. The operating point with the output current i_2 of 4.75 A is adopted for comparisons. Fig. 6 shows the transient dynamic response of the PI control and the proposed method when the output current changes between 4.75 A and 5.7 A. In the PI control, although the output voltage has no steady-state error due to the integral compensator with optimal gains, the output voltage has an undershoot and overshoot of 0.5 V. Meanwhile, in the proposed method, the output voltage shows an excellent transient dynamic response. This is because the proposed method can provide the predicted phase-shift angle accurately after every sampling period.

An experimental prototype setup is implemented with all parameters to be the same as in the simulation, where LCR meter (Agilent) is used to measure the passive parameters as L_k = 51 μH and C_2 = 219 μF, which serve as actual values.

Experimental results of the effects of parameter mismatches in the deadbeat control without parameter identification with the proposed parameter identification method are shown in Figs. 7(a) and (b), respectively. The results are almost the same as in simulations. In Fig. 7(b), the initial L_k and C_2 are purposely set to 80% of the actual values. When the proposed method is applied, the output voltage traces the reference value quickly, and parameters L_k and C_2 become equal to the actual parameter values. As a result, this proves the benefits of the proposed method.

V. Conclusion

In this paper, the LSA method is adopted for parameter identification in the deadbeat control under SPS modulation of the DAB converter. The steady-state performance is improved and actual values of L_k and C_2 are precisely identified within a few sampling periods. Besides, the proposed method is compared with the conventional PI control, where the other benefits of the proposed method are realized with excellent transient dynamic responses. Note that the proposed method can be extended to other modulation schemes such as EPS, DPS, or TPS that have more versatility.

Acknowledgment

This work was supported by the National Research Foundation of Korea (NRF) grant funded by the Korea government (MSIT) (NRF – 2020R1A2C2009303).

References

[1] L. Rui-Hao, S. Yu-Kun, and J. Xiao-Fu, "Battery state of charge estimation for electric vehicle based on neural network," in *2011 IEEE 3rd International Conference on Communication Software and Networks*, 2011, pp. 493–496.

[2] B. Zhao, Q. Song, W. Liu, and Y. Sun, "Overview of dual-active-bridge isolated bidirectional DC-DC converter for high-frequency-link power-conversion system," *IEEE Trans. Power Electron.*, vol. 29, no. 8, pp. 4091–4106, 2014.

[3] S. S. Shah and S. Bhattacharya, "Control of active component of current in dual active bridge converter," *IEEE Appl. Power Electron. Conf. Expo.*, pp. 323–330, 2018.

[4] R. K. Behera and O. Ojo, "Modeling and control of DAB converter for solar micro-grid application," *Int. Conf. Power Electron. Syst. Appl. Electr. Transp. - Automotive, Vessel Aircr.*, 2016.

[5] V. M. Iyer, S. Gulur, and S. Bhattacharya, "Small-signal stability assessment and active stabilization of a bidirectional battery charger," *IEEE Trans. Ind. Appl.*, vol. 55, no. 1, pp. 563–574, 2019.

[6] W. Zhao, X. Zhang, S. Gao, and M. Ma, "Improved Model-Based Phase-Shift Control for Fast Dynamic Response of Dual-Active-Bridge," *IEEE J. Emerg. Sel. Top. Power Electron.*, vol. 9, no. 1, pp. 223–231, 2021.

[7] Z. Ji, Q. Wang, D. Li, and Y. Sun, "Fast DC-bias current control of dual active bridge converters with feedforward compensation," *IEEE Trans. Circuits Syst. II Express Briefs*, vol. 67, no. 11, pp. 2587–2591, 2020.

[8] Q. Xiao, L. Chen, H. Jia, P. W. Wheeler, and T. Dragicevic, "Model Predictive Control for Dual Active Bridge in Naval DC Microgrids Supplying Pulsed Power Loads Featuring Fast Transition and Online Transformer Current Minimization," *IEEE Trans. Ind. Electron.*, vol. 67, no. 6, pp. 5197–5203, 2020.

[9] L. Chen, S. Shao, Q. Xiao, L. Tarisciotti, P. W. Wheeler, and T. Dragičević, "Model Predictive Control for Dual-Active-Bridge Converters Supplying Pulsed Power Loads in Naval DC Micro-Grids," *IEEE Trans. Power Electron.*, vol. 35, no. 2, pp. 1957–1966, 2020.

[10] Y. Shan, J. Hu, K. W. Chan, Q. Fu, and J. M. Guerrero, "Model Predictive Control of Bidirectional DC-DC Converters and AC/DC Interlinking Converters-A New Control Method for PV-Wind-Battery Microgrids," *IEEE Trans. Sustain. Energy*, vol. 10, no. 4, pp. 1823–1833, 2019.

[11] F. An, W. Song, B. Yu, and K. Yang, "Model predictive control with power self-balancing of the output parallel DAB DC-DC converters in power electronic traction transformer," *IEEE J. Emerg. Sel. Top. Power Electron.*, vol. 6, no. 4, pp. 1806–1818, 2018.

[12] N. Vazquez and M. Liserre, "Peak current control and feed-forward compensation of a DAB converter," *IEEE Trans. Ind. Electron.*, vol. 67, no. 10, pp. 8381–8391, 2020.

[13] F. An, W. Song, K. Yang, S. Yang, and L. Ma, "A simple power estimation with triple phase-shift control for the output parallel DAB DC-DC converters in power electronic traction transformer for railway locomotive application," *IEEE Trans. Transp. Electrif.*, vol. 5, no. 1, pp. 299–310, 2019.

[14] B. Zhao, Q. Song, W. Liu, and W. Sun, "Current-stress-optimized switching strategy of isolated bidirectional DC-DC converter with dual-phase-shift control," *IEEE Trans. Ind. Electron.*, vol. 60, no. 10, pp. 4458–4467, 2013.

[15] F. An, W. Song, and K. Yang, "Direct power control of dual-active-bridge dc–dc converters based on unified phase shift control," *J. Eng.*, vol. 2019, no. 16, pp. 2180–2184, 2019.

[16] F. An, W. Song, K. Yang, N. Hou, and J. Ma, "Improved dynamic performance of dual active bridge dc-dc converters using MPC scheme," *IET Power Electron.*, vol. 11, no. 11, pp. 1–10, 2018.

[17] N. Hou, W. Song, and M. Wu, "Minimum-Current-Stress Scheme of Dual Active Bridge DC-DC Converter with Unified Phase-Shift Control," *IEEE Trans. Power Electron.*, vol. 31, no. 12, pp. 8552–8561, 2016.

[18] F. An, W. Song, K. Yang, S. Luo, and X. Feng, "Optimised power control and balance scheme for the output parallel dual-active-bridge DC-DC converters in power electronic traction transformer," *IET Power Electron.*, vol. 12, no. 9, pp. 2295–2303, 2019.

[19] F. An, W. S. Song, and K. X. Yang, "Optimised power control with extended phase shift in dual-active-bridge DC-DC converters," *Electron. Lett.*, vol. 54, no. 10, pp. 651–653, 2018.

[20] Texas Instruments, "Analog - Passive Devices Application Report," 1999.

[21] P. Wilson, *The Circuit Designer's Companion*, 3rd ed. Newnes, 2012.

[22] H. Gualous, D. Bouquain, A. Berthon, and J. M. Kauffmann, "Experimental study of supercapacitor serial resistance and capacitance variations with temperature," *J. Power Sources*, vol. 123, no. 1, pp. 86–93, 2003.

[23] A. Vidal *et al.*, "A Method for Identification of the Equivalent Inductance and Resistance in the Plant Model of Current-Controlled Grid-Tied Converters," *IEEE Trans. Power Electron.*, vol. 30, no. 12, pp. 7245–7261, 2015.

[24] T. Q. Duong and S. J. Choi, "Parameter identification for dual-phase shift modulated DAB converters," *J. Power Electron.*, vol. 21, no. 12, pp. 1866–1877, 2021.

[25] Z. Guo, Y. Luo, and K. Sun, "Parameter Identification of

the Series Inductance in DAB Converters," *IEEE Trans. Power Electron.*, vol. 36, no. 7, pp. 7395–7399, 2021.

[26] S. Kwak, U. C. Moon, and J. C. Park, "Predictive-control-based direct power control with an adaptive parameter identification technique for improved AFE performance," *IEEE Trans. Power Electron.*, vol. 29, no. 11, pp. 6178–6187, 2014.

[27] S. Wei, Z. Zhao, K. Li, L. Yuan, and W. Wen, "Deadbeat Current Controller for Bidirectional Dual-Active-Bridge Converter Using an Enhanced SPS Modulation Method," *IEEE Trans. Power Electron.*, vol. 36, no. 2, pp. 1274–1279, 2021.

[28] S. Dutta, S. Hazra, and S. Bhattacharya, "A digital predictive current-mode controller for a single-phase high-frequency transformer-isolated dual-active bridge DC-to-DC converter," *IEEE Trans. Ind. Electron.*, vol. 63, no. 9, pp. 5943–5952, 2016.

[29] L. Shi, W. Lei, Z. Li, J. Huang, Y. Cui, and Y. Wang, "Bilinear Discrete-Time Modeling and Stability Analysis of the Digitally Controlled Dual Active Bridge Converter," *IEEE Trans. Power Electron.*, vol. 32, no. 11, pp. 8787–8799, 2017.

[30] H. Qin and J. W. Kimball, "Generalized average modeling of dual active bridge DC-DC converter," *IEEE Trans. Power Electron.*, vol. 27, no. 4, pp. 2078–2084, 2012.

[31] E. K. P. Chong and S. H. Zak, *An Introduction to Optimization*, Fourth ed. Wiley, 2013.